JACS
JOURNAL OF THE AMERICAN CHEMICAL SOCIETY

Communication

pubs.acs.org/JACS

Direct Optical Determination of Interfacial Transport Barriers in Molecular Tunnel Junctions

Jerry A. Fereiro,[†] Richard L. McCreery,*[,†,‡] and Adam Johan Bergren*[,‡]

[†]Department of Chemistry, University of Alberta, Edmonton, Alberta, Canada

[‡]National Institute for Nanotechnology, National Research Council Canada, Edmonton, Alberta, Canada

Supporting Information

ABSTRACT: Molecular electronics seeks to build circuitry using organic components with at least one dimension in the nanoscale domain. Progress in the field has been inhibited by the difficulty in determining the energy levels of molecules after being perturbed by interactions with the conducting contacts. We measured the photocurrent spectra for large-area aliphatic and aromatic molecular tunnel junctions with partially transparent copper top contacts. Where no molecular absorption takes place, the photocurrent is dominated by internal photoemission, which exhibits energy thresholds corresponding to interfacial transport barriers, enabling their direct measurement in a functioning junction.

In addition to possibly representing an important size limit for miniaturization of electronic components,[1] circuit elements incorporating molecules may provide new functions or better performance than current devices.[2] The ability to make the advanced function/performance molecular components that have been envisioned is aided by specific tailoring of electronic energy levels,[3−5] which generally differ significantly from those of the isolated molecules and contact materials.[6] It is therefore critical to determine these energy levels in functioning devices in order to fully understand the factors that control the electronic properties of molecular devices.

Photocurrent measurements have been used to probe the height of interfacial barriers in classical oxide-containing tunnel junctions.[7−12] In these cases, nonequilibrium carriers generated from the decay of photoexcited surface plasmons[13] in a metal contact produce photocurrent when the incident photons have energy in excess of the interfacial barrier height in the oxide. For example, photocurrent cutoff energies can directly yield the barrier for electron or hole tunneling.[10] The generation of photocurrent in molecular devices has been considered theoretically,[14] and a few measurements of a range of photoeffects have been reported.[15−17] These have generally shown a persistent, nonbolometric photocurrent, but the observed effects have not been correlated with device energy levels.

In this contribution, we show that photocurrent observed in large-area carbon/molecule/Cu tunnel junctions can be used to determine transport parameters, including the relative alignment of molecular energy levels and the height(s) of the tunnel barrier(s). The results reported here establish a method for directly measuring the energy levels in working molecular junctions and may be used to design more advanced molecular electronic circuitry.

Charge transport in molecular junctions is governed by the height of the interfacial energy barriers, as well as the total distance between the conductors. For small distances (i.e., less than ∼5 nm[18,19]), quantum mechanical tunneling dominates transport. We have previously shown that transport in carbon/molecule/Cu molecular junctions with thickness of less than ∼5 nm (see Figure 1A for an idealized schematic of junction

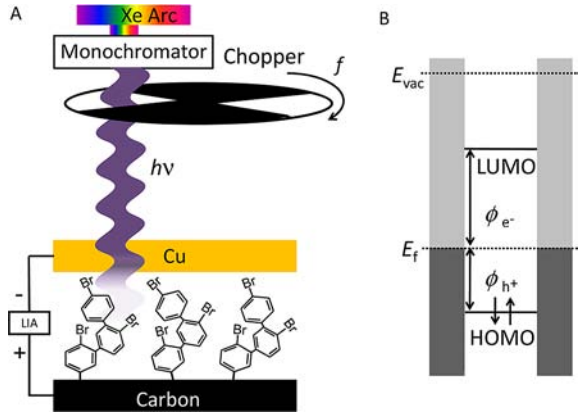

Figure 1. (A) Schematic diagram of a molecular tunnel junction illuminated by light incident on the top contact. (B) Energy level diagram showing a nonresonant tunnel barrier for holes (HOMO-mediated transport) and electrons (LUMO-mediated transport).

structure) is consistent with coherent tunneling, with very weak temperature dependence.[6,20,21] Figure 1B shows an energy level diagram of the molecular junction depicted in Figure 1A. Here, the offset between the Fermi level (E_f) of the contacts and the molecular orbital energies defines the tunneling barrier for electrons (ϕ_{e^-}, for LUMO-mediated transport) and holes (ϕ_{h^+}, for HOMO-mediated transport).

While the energy level diagram seems straightforward, the energy levels of the isolated components often cannot be used to determine the tunneling barrier in a completed device.[6,22] The failure of the Schottky−Mott rule[5,23] in carbon/molecule/Cu devices is due to strong electronic coupling between the substrate and molecule, which perturbs the energy levels such that the local vacuum levels of the substrate and molecular layer

Received: March 28, 2013
Published: June 19, 2013

   dx.doi.org/10.1021/ja403123a | J. Am. Chem. Soc. 2013, 135, 9584−9587

are not aligned. While ex situ measurements using ultraviolet photoelectron spectroscopy (UPS) can be used to estimate hole barriers[6,24] that can be correlated to transport measurements, such methods do not include the effect of the top contact. Because the entire system needs to be considered together, it is clear that a technique for direct measurement of the tunnel barrier in a completed, working molecular junction is highly desirable.

Figure 1A shows a schematic of the junction structure used in this study (details of junction fabrication, including $J-V$ curves, and photocurrent measurement can be found in Supporting Information [SI] section 2) along with a diagram of the optical and electronic apparatus. Briefly, a narrow band ($\Delta\lambda$ = 13 nm) of light from a Xe arc source passes through an optical chopper before incidence onto the junction. Phase-sensitive lock-in detection is used to measure the resulting photocurrent, including the sign, which is converted to yield by calibration of the incident power (see SI sections 3, 4). The system permitted measurement of photocurrent from carbon/molecule/Cu junctions with 20 nm thick partially transparent Cu contacts.

Figure 2 shows a plot of yield (Y) vs energy for two molecular junctions (carbon/molecule/with 20 nm Cu top

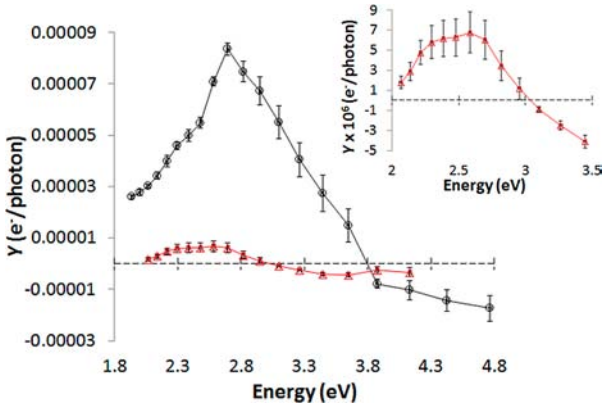

Figure 2. Yield vs energy for BrP (○, black) and C12 (△, red) molecular junctions, along with an inset to show the alkane junction in greater detail. The y-axis error bars are ± one standard deviation for four (BrP) or six (C12) junctions, and the band-pass of the monochromator is 13 nm (x-axis error bars are smaller than the data points). See SI Section 1 for a plot with wavelength as the abscissa.

contacts): bromophenyl (BrP, 3.0 nm thick multilayer) and aminododecane (C12, 2.3 nm). Differences are observed in the shape of the spectra for the two molecules (see also inset). This is a preliminary indication that the response is dependent on molecular structure (and associated energy levels) and is not due to heating effects or other artifacts (see SI sections 5, 6). In addition, as shown in SI section 6, when a junction that does not contain a molecule (i.e., a direct PPF/Cu contact) is illuminated, the response obtained is indistinguishable from the dark response. Overall, the response obtained from molecular junctions is consistent with internal photoemission (IPE), where hot carriers generated in the Cu top contact can cross the interfacial tunneling barrier, as discussed below.

IPE has been described as a subwork function photoelectric effect, where the charge carriers are excited from one conductor into another across a solid-state barrier material rather than into a vacuum (which would require a higher energy than barrier crossing).[25] In the carbon/molecule/Cu devices employed here, IPE might involve optically generated carriers in the top Cu metal crossing the molecular layer and passing into the underlying carbon substrate to generate a photocurrent. Generally, internal photoemission yield (Y) is governed by Fowler theory such that under the conditions employed:[25−27]

$$Y \alpha (E - \phi)^2 \quad (1)$$

where E is the incident photon energy ($h\nu$, where h is Planck's constant and ν is frequency), and ϕ is the interfacial barrier (here, a tunneling barrier).

Considering eq 1, a plot of $Y^{1/2}$ versus photon energy (i.e., a Fowler plot) is expected to be linear if IPE is the only process involved in photocurrent generation. Linear extrapolation of the Fowler plot to the x-axis can be used to estimate the value of the interfacial barrier height. The generation of charge carriers in the Cu follows excitation and decay of surface plasmons, generating both electrons and holes with excess energy. These hot carriers can therefore cross both electron and hole tunneling barriers,[25] resulting in either positive or negative photocurrents and serving as a possible indication of the position of both occupied and unoccupied states in the barrier region.

Figure 3A shows Fowler plots for the positive photocurrent region. From Figure 1, a positive photocurrent in the external

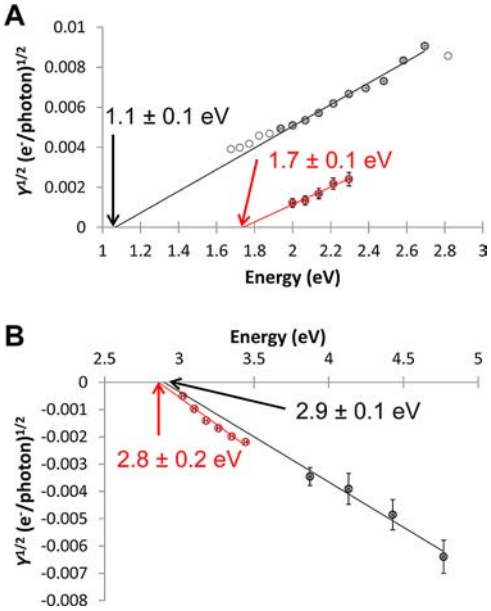

Figure 3. (A) Fowler plot for two different junctions where positive photocurrent is observed at PPF. (B) Fowler plot for negative photocurrent for the same two junctions. Extrapolated thresholds for each case are given.

circuit is observed when an electron is transferred from the carbon to a photogenerated hole in the top Cu contact via the molecular HOMO. Both Fowler plots display good linearity, indicating that an IPE model fits well with the experimental data. In addition, the slopes of these plots are similar, indicating that the energetic distribution of optically generated charge carriers is similar. Finally, the extrapolated barrier heights for holes (ϕ_{h+}) obtained from the Fowler plots in Figure 3A are 1.1 eV for BrP and 1.7 eV for C12, respectively. Given the error in the measurements (±0.1 eV), these values are clearly statically different from each other, demonstrating a structural effect on the barrier for hole tunneling in molecular junctions. In

dx.doi.org/10.1021/ja403123a | J. Am. Chem. Soc. 2013, 135, 9584−9587

addition, these results are supported by measurements of $E_{HOMO,onset}$ energies determined using UPS and $J-V$ curve fitting,[21] where $E_{HOMO,onset}$ for C12 is 1.7 eV and that for BrP is 1.2 ± 0.3 eV (see SI section 7). Thus, the optical method used here indicates that changes in the barrier height resulting from differences in molecular structure can be determined by using photocurrent measurements. However, the optical method is conducted in situ, resulting in a barrier value for a functioning molecular junction with a top contact, while UPS can probe only the occupied states of a carbon/molecule system lacking a top contact, in vacuum.

While UPS can only determine the energy onset of the occupied states, IPE may be sensitive to both electron and hole barriers.[25] Determination of the sign of the dominant tunneling carrier has been a long-standing issue in molecular electronics. A few studies have reported values either through ex situ photoelectron measurements[28,29] or observation of the thermoelectric effect.[30,31] However, in some cases, IPE may yield the dominant carrier sign as well as the values of tunneling barriers for both carrier types, as shown below.

Figure 3B shows the Fowler plot for the high-energy region where the measured photocurrent is negative (here, the y-axis is $-[|Y|^{1/2}]$). These plots show good linearity and yield electron tunneling barriers of 2.9 and 2.8 eV for C12 and BrP, respectively. While the interpretation of these data may be used to construct energy level diagrams (as discussed below), we first comment on the mechanism involved in photocurrent generation and the implicit assumptions in the model, as well as alternative possibilities.

Figure 4 shows a schematic diagram of IPE for hole (Figure 4A) and electron (Figure 4B) current for photoexcitation

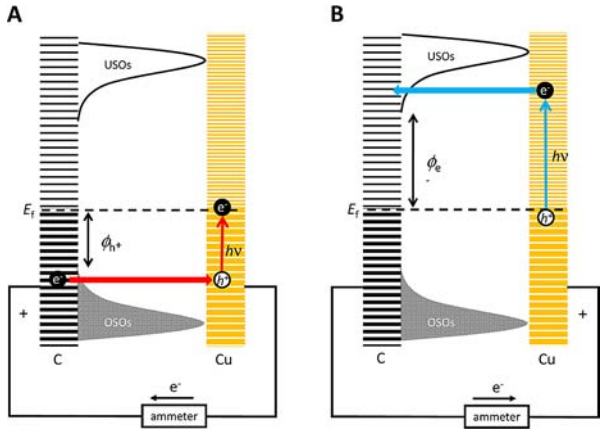

Figure 4. (A) Diagram of the IPE mechanism for excitation of holes from Cu to carbon. (B) Diagram for electron transport from Cu to carbon. The alignment of the occupied system orbitals (OSOs) and unoccupied system orbitals (USOs) relative to the contact Fermi levels determines the sign of the observed photocurrent and the energy threshold for onset.

exclusively in the Cu electrode. As shown in Figure 4A, low-energy light incident onto the Cu top contact creates electron–hole pairs with an energy defined by the photon energy. Thus, the deepest hole has an energy = $(E_f - h\nu)$, and when this is larger than the hole tunneling barrier, HOMO-mediated transport of an electron from the bottom carbon contact into the hole created in the Cu can lead to a positive photocurrent in the external circuit. As shown in Figure 4B, higher-energy excitation may lead to LUMO-mediated transport when the value $(E_f + h\nu)$ exceeds the LUMO level, giving a negative photocurrent. In this model, it is implicit that excitons are generated in the Cu only, and not in the carbon. Note that if photoexcitation takes place in the carbon contact, then a negative current may be recorded at the carbon when an electron tunnels from the Cu into the PPF as a result of holes generated at $(E_f - h\nu)$. Thus, the "reverse" of the diagram in Figure 4A is possible, and will counteract a portion of the current induced by absorption in Cu. In addition, it is assumed here that there is no light-induced excitation of the molecular component, which we address next.

To determine the effect of molecular absorption on the photocurrent, the absorption spectra of the molecules bonded to a transparent carbon support were obtained (see SI section 8). These results showed that the alkane molecules are nonabsorbing throughout the entire energy range tested, while the BrP molecule shows no significant absorbance below ~3.8 eV. Thus, photoexcitation of BrP molecules is unlikely for energies up to 3.8 eV. However, the response for the BrP junction at higher energies may be due to "pseudo-IPE" currents generated by a mechanism involving molecular absorption.[25] In this case the interpretation of the threshold exhibited in the Fowler plot at high energy may need to be modified.

Table 1 lists the values of hole and electron barriers for both molecular junctions, assuming that only IPE proceeding from

Table 1. List of Barriers Determined Using IPE

junction	ϕ_{h+} (eV)	ϕ_{e-} (eV)
C/NH$(CH_2)_{11}CH_3$(2.3)/Cu(20)	1.7 ± 0.1	2.8[a]
C/BrP(3.0)/Cu(20)	1.1 ± 0.1	2.9[a]

[a]These values assume unidirectional IPE and no optical absorption by the molecular layer (see text).

the Cu generates photocurrent. Note that the HOMO and LUMO levels are not those for isolated molecules but instead are the occupied system orbitals (OSOs) and unoccupied system orbitals (USOs). Accordingly, these are drawn as a distribution of states below and above E_f in Figure 4, where the onset of photoemission represents the edges of these states becoming energetically accessible. Using this model, and considering IPE in both directions, the initial onset of photocurrent represents the most energetically accessible state, enabling at least the unambiguous determination of the smallest tunneling barrier in the system. However, the HOSO–LUSO gap determined using IPE does not directly reflect the HOMO–LUMO gap of the isolated molecule used in the junction, but rather the transport gap of the system relevant to determining the tunneling barriers. This distinction is important, as the IPE observed here yields information regarding a completed junction, including the results of any interactions between the molecules and contacts, which tend to decrease the energy gap.[5]

Turning to a comparison of the results, we note that the alkane-based junction has a larger energy gap than the aromatic junction (4.5 vs 4.0 eV), consistent with the decreased conductivity in previous measurements.[32] The absolute value for the transport gap of the alkane junction as assessed here is smaller than other reported values,[29] which range from 7 to 8 eV, with tunneling barriers of 3–4 eV. However, as recently summarized,[33] the barrier heights reported for alkane-containing junctions using other paradigms is often less than

dx.doi.org/10.1021/ja403123a | J. Am. Chem. Soc. 2013, 135, 9584–9587

2 eV,[34−36] suggesting a lower transport gap. These different results illustrate that the details of the system (i.e., contact materials and interactions between the contacts and molecules) affect the transport barrier. Given that the system studied here has strong electronic coupling between the molecules and substrate, the reduced gap may be due to an induced density of interface states,[37,38] sometimes referred to as gap states,[4] which are transport states lying within the HOMO−LUMO gap of the molecular species. A distribution of such gap states may be sufficient to cause a lowering of the transport gap.

This work has shown that photocurrent measurements of completed carbon/molecule/Cu junctions can yield valuable information about energy level alignment. An IPE mechanism was shown to be useful for determining both electron and hole tunneling barriers for a complete and operational carbon/alkane/Cu molecular junction. For the aromatic molecule bromophenyl, a hole tunneling barrier lower than that for the alkane was obtained. The values of the hole tunneling barriers agree well with recent measurements of $E_{HOMO,onset}$ values obtained with UPS. Although IPE currents induced in both contacts may contribute to the observed response, the threshold for photocurrent generation directly indicates the smallest tunneling barrier in the molecular junction, and this barrier is the most likely to determine the charge transport characteristics of the device. In addition, pseudo-IPE current may add to the photocurrent at higher photon energies for molecules that show optical absorbance. This additional mechanism is directly related to the molecular component, and we anticipate significant information to be gained by analysis of both IPE and pseudo-IPE portions of the photocurrent spectrum.

■ ASSOCIATED CONTENT

Supporting Information

Detailed descriptions of the experimental setup, calibration, optical spectra, molecular layer thickness measurements, assessments of reproducibility, and other details are given in Supporting Information. This material is available free of charge via the Internet at http://pubs.acs.org.

■ AUTHOR INFORMATION

Corresponding Author

richard.mccreery@ualberta.ca (R.L.M.); adam.bergren@nrc.ca (A.J.B.)

Notes

The authors declare no competing financial interest.

■ ACKNOWLEDGMENTS

This work was supported by the University of Alberta, the National Research Council and Natural Science and Engineering Research Council of Canada, and the Province of Alberta through NanoBridge. We thank Nikola Pekas and Jillian Buriak for valuable discussions, Bryan Szeto for expert assistance with LabView programming, and Sayed Youssef Sayed for assistance with fabrication of alkane junctions.

■ REFERENCES

(1) Carroll, R. L.; Gorman, C. B. *Angew. Chem., Int. Ed.* **2002**, *41*, 4378.
(2) McCreery, R. L.; Bergren, A. J. *Adv. Mater.* **2009**, *21*, 4303.
(3) Ishii, H.; Sugiyama, K.; Ito, E.; Seki, K. *Adv. Mater.* **1999**, *11*, 605.
(4) Zhong, S.; Zhong, J. Q.; Mao, H. Y.; Zhang, J. L.; Lin, J. D.; Chen, W. *Phys. Chem. Chem. Phys.* **2012**, *14*, 14127.
(5) Braun, S.; Salaneck, W. R.; Fahlman, M. *Adv. Mater.* **2009**, *21*, 1450.
(6) Sayed, S. Y.; Fereiro, J. A.; Yan, H.; McCreery, R. L.; Bergren, A. J. *Proc. Natl. Acad. Sci. U.S.A.* **2012**, *109*, 11498.
(7) Powell, R. *J. Appl. Phys.* **1970**, *41*, 2424.
(8) Gundlach, K. H.; Kadlec, J. *J. Appl. Phys.* **1975**, *46*, 5286.
(9) DiMaria, D. J.; Arnett, P. C. *Appl. Phys. Lett.* **1975**, *26*, 711.
(10) Goodman, A. M. *J. Appl. Phys.* **1970**, *41*, 2176.
(11) Deal, B. E.; Snow, E. H. J. *Phys. Chem. Solids* **1966**, *27*, 1873.
(12) Kovacs, D. A.; Winter, J.; Meyer, S.; Wucher, A.; Diesing, D. *Phys. Rev. B* **2007**, *76*, 235408.
(13) Campbell, I. H.; Smith, D. L. *In Conjugated Polymer and Molecular Interfaces: Science and Technology for Photonic and Optoelectronic Applications*; Salaneck, W. R., Seki, K., Kahn, A., Pireaux, J.-J., Eds.; Marcel Dekker: New York, 2002, p 693.
(14) Galperin, M.; Nitzan, A. *Phys. Chem. Chem. Phys.* **2012**, *14*, 9421.
(15) Mangold, M. A.; Calame, M.; Mayor, M.; Holleitner, A. W. *J. Am. Chem. Soc* **2011**, *133*, 12185.
(16) Huang, W.; Masuda, G.; Maeda, S.; Tanaka, H.; Ogawa, T. *Chem.—Eur. J.* **2006**, *12*, 607.
(17) Battacharyya, S.; Kibel, A.; Kodis, G.; Liddell, P. A.; Gervaldo, M.; Gust, D.; Lindsay, S. *Nano Lett.* **2011**, *11*, 2709.
(18) Choi, S. H.; Kim, B.; Frisbie, C. D. *Science* **2008**, *320*, 1482.
(19) Choi, S. H.; Risko, C.; Delgado, M. C. R.; Kim, B.; Bredas, J.-L.; Frisbie, C. D. *J. Am. Chem. Soc.* **2010**, *132*, 4358.
(20) Bergren, A. J.; McCreery, R. L.; Stoyanov, S. R.; Gusarov, S.; Kovalenko, A. *J. Phys. Chem. C* **2010**, *114*, 15806.
(21) Yan, H.; Bergren, A. J.; McCreery, R. L. *J. Am. Chem. Soc.* **2011**, *133*, 19168.
(22) Salomon, A.; Boecking, T.; Seitz, O.; Markus, T.; Amy, F.; Chan, C.; Zhao, W.; Cahen, D.; Kahn, A. *Adv. Mater.* **2007**, *19*, 445.
(23) McCreery, R. L.; Yan, H.; Bergren, A. J. *Phys. Chem. Chem. Phys.* **2013**, *15*, 1065.
(24) Kim, B.; Choi, S. H.; Zhu, X. Y.; Frisbie, C. D. *J. Am. Chem. Soc.* **2011**, *133*, 19864.
(25) Afanas'ev, V. V. *Internal Photoemission Spectroscopy: Principles and Applications*; Elsevier: New York, 2008.
(26) Sze, S. M. *Physics of Semiconductor Devices*; 2nd ed.; Wiley: New York, 1981.
(27) Fowler, R. H. *Phys. Rev.* **1931**, *38*, 45.
(28) Yaffe, O.; Qi, Y.; Scheres, L.; Puniredd, S. R.; Segev, L.; Ely, T.; Haick, H.; Zuilhof, H.; Vilan, A.; Kronik, L.; Kahn, A.; Cahen, D. *Phys. Rev. B* **2012**, *85*, 045433.
(29) Qi, Y.; Yaffe, O.; Tirosh, E.; Vilan, A.; Cahen, D.; Kahn, A. *Chem. Phys. Lett.* **2011**, *511*, 344.
(30) Reddy, P.; Jang, S.-Y.; Segalman, R. A.; Majumdar, A. *Science* **2007**, *315*, 1568.
(31) Malen, J. A.; Doak, P.; Baheti, K.; Tilley, T. D.; Segalman, R. A.; Majumdar, A. *Nano Lett.* **2009**, *9*, 1164.
(32) Salomon, A.; Cahen, D.; Lindsay, S.; Tomfohr, J.; Engelkes, V. B.; Frisbie, C. D. *Adv. Mater.* **2003**, *15*, 1881.
(33) Niskala, J. R.; Rice, W. C.; Bruce, R. C.; Merkel, T. J.; Tsui, F.; You, W. *J. Am. Chem. Soc* **2012**, *134*, 12072.
(34) Wang, G.; Kim, T.-W.; Jo, G.; Lee, T. *J. Am. Chem. Soc* **2009**, *131*, 5980.
(35) Li, X.; He, J.; Hihath, J.; Xu, B.; Lindsay, S. M.; Tao, N. *J. Am. Chem. Soc.* **2006**, *128*, 2135.
(36) Engelkes, V. B.; Beebe, J. M.; Frisbie, C. D. *J. Am. Chem. Soc.* **2004**, *126*, 14287.
(37) Shen, C.; Kahn, A. *Org. Electron.* **2001**, *2*, 89.
(38) Segev, L.; Salomon, A.; Natan, A.; Cahen, D.; Kronik, L. *Phys. Rev. B* **2006**, *74*, 165323.